Histol Histopathol (2020) 35: 457-474

http://www.hh.um.es

Histology and Histopathology
From Cell Biology to Tissue Engineering

Histology of skeletal muscle reconstructed by means of the implantation of autologous adipose tissue: an experimental study

Fernando Leiva-Cepas[1,2,3]*, Ignacio Jimena[1,2,3], Ignacio Ruz-Caracuel[1,2#], Evelio Luque[1,3], Rafael Villalba[4] and Jose Peña-Amaro[1,2,3]

[1]Department of Morphological Sciences, Section of Histology, Faculty of Medicine and Nursing, [2]Research Group in Muscle Regeneration, [3]Maimonides Institute for Biomedical Research IMIBIC, Reina Sofia University Hospital, University of Cordoba and [4]Tissue of Establishment of the Center for Transfusion, Tissues and Cells, Cordoba, Spain

Present address: *Department of Pathology, Reina Sofia University Hospital, Cordoba, #Department of Pathology, Ramón y Cajal University Hospital, Madrid, Spain

Summary. The purpose of this study was to determine the histological characteristics of a skeletal muscle reconstructed by means of the implantation of autologous adipose tissue following an experimentally-induced volumetric muscle loss. A cylindrical piece in the belly of the rat anterior tibial muscle was removed. In the hole, inguinal subcutaneous adipose tissue of the same rat was grafted. Animals were sacrificed 7, 14, 21, 28 and 60 days posttransplantation. Histological, histochemical, immunohistochemical and morphometric techniques were used. At all times analyzed, the regenerative muscle fibers formed from the edges of the muscle tissue showed histological, histochemical and immunohistochemical differences in comparison with the control group. These differences are related to delays in the maturation process and are related to problems in reinnervation and disorientation of muscle fibers. The stains for MyoD and desmin showed that some myoblasts and myotubes seem to derive from the transplanted adipose tissue. After 60 days, the transplant area was 20% occupied by fibrosis and by 80% skeletal muscle. However, the neo-muscle was chaotically organized showing muscle fiber disorientation and centronucleated fibers with irregular shape and size. Our results support the hypothesis that, at least from a morphological point of view, autologous adipose tissue transplantation favors reconstruction following a volumetric loss of skeletal muscle by combining the inherent regenerative response of the organ itself and the myogenic differentiation of the stem cells present in the adipose tissue. However, in our study, the formed neo-muscle exhibited histological differences in comparison with the normal skeletal muscle.

Key words: Skeletal muscle, Muscle regeneration, Adipose tissue, Graft, Fibrosis

Offprint requests to: Jose Peña, Departamento de Ciencias Morfológicas (Seccion de Histología), Facultad de Medicina y Enfermería, Universidad de Córdoba, Cordoba, Spain. e-mail: cm1peamj@uco.es

DOI: 10.14670/HH-18-163

Introduction

The skeletal muscles have a great capacity to regenerate after injury (Huard et al., 2002). However, in severe injuries such as volumetric muscle loss (VML), this capacity is insufficient, and the injury progresses into muscle fibrosis (Garg et al., 2014; Cholok et al., 2017). Strategies aimed at stimulating the *de novo* formation of skeletal muscle tissue as a treatment in cases of VML must therefore be developed in the field of regenerative medicine (Turner and Badylak, 2012; Cittadella-Vigodarzere and Mantero, 2014; Sicari et al., 2014; Grasman et al., 2015; Corona et al., 2016). Several *in vitro* and *in vivo* studies including different

combinations of stem cells, biomaterials, and growth factors have been carried out in the field of skeletal muscle tissue engineering techniques (Qazi et al., 2015; Fuoco et al., 2016; Kwee and Mooney, 2017; Liu et al., 2018; Pantelic and Larkin, 2018), but the muscles designed by means of tissue engineering do not achieve a natural volumetric efficiency, particularly in terms of their thickness and strength (Ostrovidov et al., 2014). Thus, the ability to form neo-muscle is limited and based on the generation of "islands" of regenerative (Aurora et al., 2015; Corona and Greising, 2016) or incipient fibers that are thinner and shorter than the native muscle fibers (Kesireddy, 2016). The possibility of implementing autologous transplantations for the treatment of VML has focused on the use of autologous minced muscle grafts on the basis that these include myogenic cells from the donor (Corona et al., 2013, 2017; Ward et al., 2015). While these procedures have achieved remarkable *de novo* muscle regeneration, it appears that the amount needed to repair VML constitutes a limitation (Dunn et al., 2019).

Following birth, the main source of mesenchymal stem cells with applications in regenerative medicine is adipose tissue (Mizuno et al., 2002; Gomillion and Burg, 2006; Schäffler and Büchler, 2007; Mizuno 2010; Argentati et al., 2018). There is *in vitro* evidence of the myogenic conversion of stem cells derived from this tissue (Di Rocco et al., 2006; Andersen et al., 2008). Also, *in vivo* these cells can contribute to muscle regeneration in mice with muscular dystrophy (*mdx*) and normal regeneration induced by myotoxins (Bacou et al., 2004; Andersen et al., 2008). However, the combination of adipose-derived stem cells with scaffolds appears to contribute to a moderate degree to the generation of new muscle fibers (Kesireddy, 2016; Gilbert-Honick et al., 2018).

In this study we hypothesized that the implantation of autologous adipose tissue directly into the area of VML might favor muscle regeneration. Our approach is based on the following aspects: i) that myoblasts can invade an area of the adipose tissue implanted in an injury, growing inwards from the edges of the severed muscle and forming myotubes throughout it (Satoh et al., 1992); and ii), that the adipose tissue stem cells may promote muscle reconstruction, as it is a well-known fact that the muscular environment has significant effects on the destination of the resident or implanted cells (Long 2001; Peng and Huard, 2004; Ehrhadt and Morgan, 2005) due to the fact that the regenerating muscle is a rich source of signals that recruit cells for the myogenesis process (De Angelis et al., 1999).

Given the above, in this study we used the implantation of adipose tissue as a means to reconstruct a muscle mass volume defect considering the fact that the myogenic potential of the cells present in the adipose tissue could be stimulated *in vivo* to favor the reconstruction of the injured muscle. Our results support the hypothesis that, at least from a morphological point of view, autologous adipose tissue transplantation favors reconstruction following a volumetric loss of skeletal muscle by combining the inherent regenerative response of the organ itself and the myogenic differentiation of the stem cells present in the adipose tissue.

Materials and methods

Experimental animals

A total of 64 Wistar rats weighing approximately 250±50 g were used in this study under controlled temperature (22±3°C) and illumination (cycles of 12 h of light and 12 h of darkness) conditions, as well as with *ad libitum* access to food (Purina®, Barcelona, Spain) and water. All procedures were carried out in accordance with Directive 2010/63/EU of the European Council and Parliament (22 September 2010) governing the protection and use of animals for scientific purposes. The study was approved by the Animal Experimentation Ethics Committee (AEEC) of the University of Cordoba (Spain).

The animals were categorized into four groups: (i) a "normal" group (N) comprised by normal rats (n=4) that did not undergo any intervention; (ii) a "myotoxin-injured" group (MI) comprised by rats (n=20) that had a myotoxin injected into their anterior tibial (AT) muscle and were used as a control of the normal regenerative process (Biérinx and Sebille, 2008); (iii) an adipose graft (AG) group comprised by rats (n=20) that had autologous adipose tissue implanted in a VML defect induced in their AT muscle; and (iv), a "frozen adipose graft" (FAG) group comprised by rats (n=20) that had autologous adipose tissue which had previously been subjected to freeze-thawing cycles (3 repetitive cycles of direct immersion in liquid nitrogen (-196°C) performed in a total period of three minutes) in order to achieve total destruction of the cells (Shier, 1988) implanted in the induced VML defect and were used as a comparison group for the previous one.

Experimental and surgical procedures

All surgical procedures were performed under anesthesia and in aseptic conditions. To induce the degeneration-regeneration of the muscle tissue in the MI group, the rats had 100 μl of mepivacaine hydrochloride 2% (Scandinibsa; Inibsa, Barcelona, Spain) injected into the central area of the AT muscle through a fine needle. To induce the VML defect in the AG and FAG groups, the AT muscles were exposed, and a sterile punch (6 mm in diameter and 5 mm in length) was used to perform a biopsy, obtaining a cylindrical fragment of tissue from the central portion of the belly of the left AT muscle. Subcutaneous adipose tissue obtained from the inguinoabdominal region of the same specimen was then implanted into the muscle defect (Fig. 1a-c). The amount extracted from autologous adipose tissue was similar to the muscle fragment (approximately 0.07 g). Both surgical sites were finally cleaned, disinfected, and

sutured, and each rat was orally administered 20 mg/kg of post-surgical ceftriaxone that was diluted in their drinking water.

The animals were subsequently sacrificed at 7, 14, 21, 28, and 60 days postinjection (normal regeneration group, MI) and post-implantation (AG and FAG adipose tissue groups). Their AT muscles were then extracted and processed to perform histological, histochemical, and immunohistochemical analyses.

Sample processing

The muscle bellies were extracted and placed on small cork sheets using the OCT compound® (Tissue Tek, Japan), oriented in such a way as to obtain cross sections. The samples were quickly frozen in isopentane (2-methylbutane; Sigma-Aldrich, St. Louis, MO, USA), cooled in liquid nitrogen, and cross sections with a thickness of 8 μm were obtained using a cryostat (Leica CM1850 UV, Leica Microsystems, Nussloch, Germany) set at a temperature of -20°C.

Histological, histochemical, and immunohistochemical techniques

Standard protocols used for the microscopic study of skeletal muscle were followed (Dubowitz et al., 2013). To perform the general morphological evaluation, the samples were stained with hematoxylin and eosin (H&E) and modified Gomori trichrome (mGT). The histochemical techniques applied included the use of nicotinamide adenosine dinucleotide-tetrazolium reductase (NADH-tr), ATPase ph 9.4, acid phosphatase, oil Red O, and acridine orange (AO). Immunostaining was performed using the following primary antibodies: desmin (1:100, clone D33, Dako®), MyoD (1:50, clone 58A, Dako®) and laminin (1:50, clone 4C7, Dako®). Briefly, after a 5 minutes acetone fixation, primary antibodies were incubated for 2 hours. Visualization was performed using the LSAB+System-HRP (K0979, Dako, Denmark) following the manufacturer's instructions. Negative controls were performed in parallel without primary antibodies. Nuclei counterstaining was performed with Mayer's hematoxylin.

Histomorphometry

Micrographs were obtained with a Nikon Eclipse E1000 microscope (Nikon, Tokyo, Japan) incorporating a Sony DXC-990P (Sony, Tokyo, Japan) color video camera. Fluorescence images of the samples stained with AO were taken using a Leitz Orthoplan microscope.

The images obtained for the morphometric analysis were then transferred to a computer equipped with the Image-Pro Plus 6.5 image analysis software (Media Cybernetics, Bethesda, MA, USA). Five areas within the

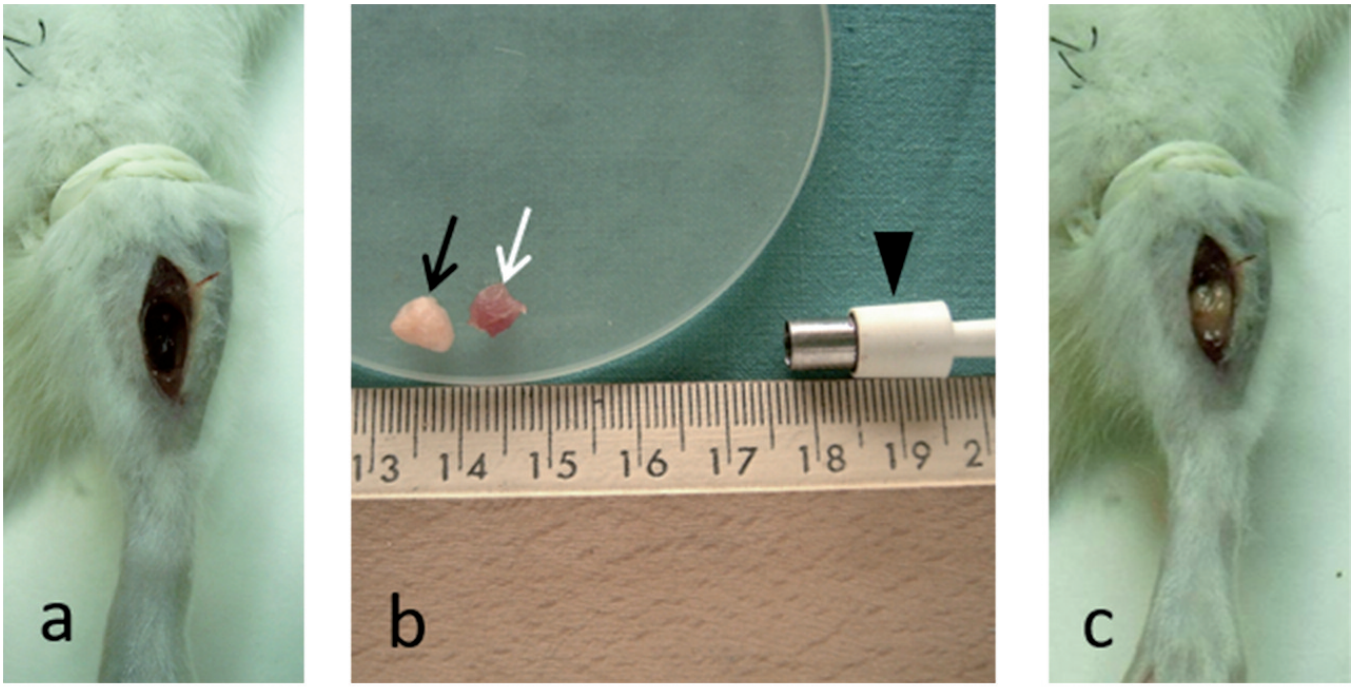

Fig. 1. Procedure followed for the reconstruction of an area of VML induced in the AT muscle using an autologous adipose tissue transplant. **a.** Defect caused in the middle third of the muscle. **b.** Muscle fragment (white arrow) and fragment of autologous adipose tissue (black arrow) extracted from the inguinal region; punch used to cause the muscular defect (arrowhead). **c.** Adipose tissue implanted in the area of VML.

implantation site were photographed in the 60-day groups using cross-sectional magnifications of approximately 40x of each muscle stained with H&E. The following parameters were examined in each area: the number of fibers, the cross-sectional area of the fibers, the number of regenerated muscle fibers (containing nuclei in a central location), the number of disoriented fibers, and the percentage of fibrous tissue (the area covered by collagen staining was evaluated in terms of the percentage of the total picture area).

Statistical analysis

The data were analyzed using statistical software SigmaStat 3.1. To perform the statistical analysis, the mean of the five areas was calculated for each specimen, and the mean ± standard deviation was then obtained for each group. The Holm-Sidak t-test or Dunn' test was

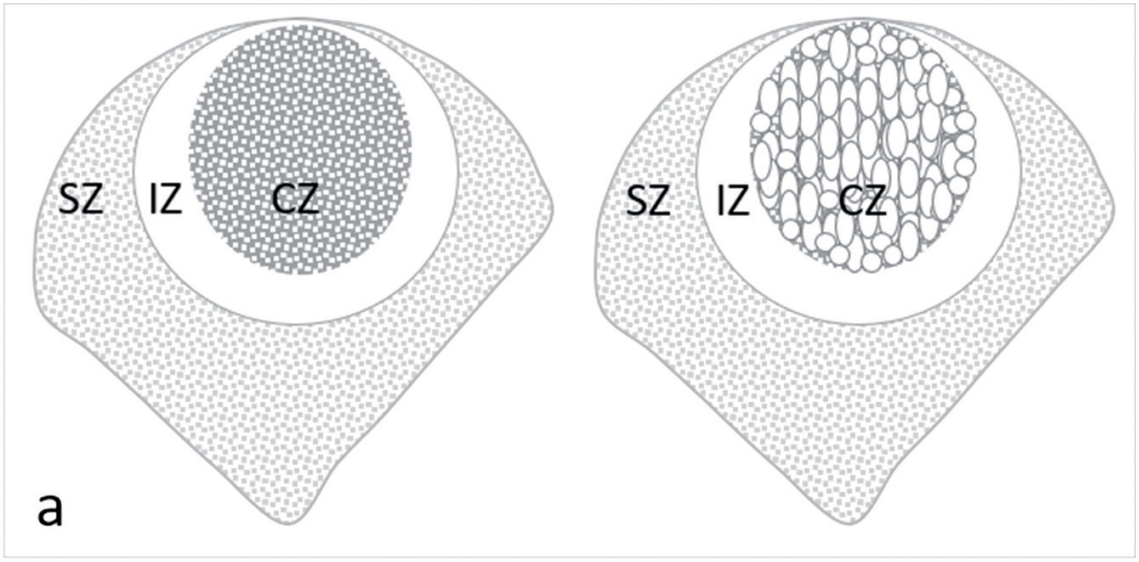

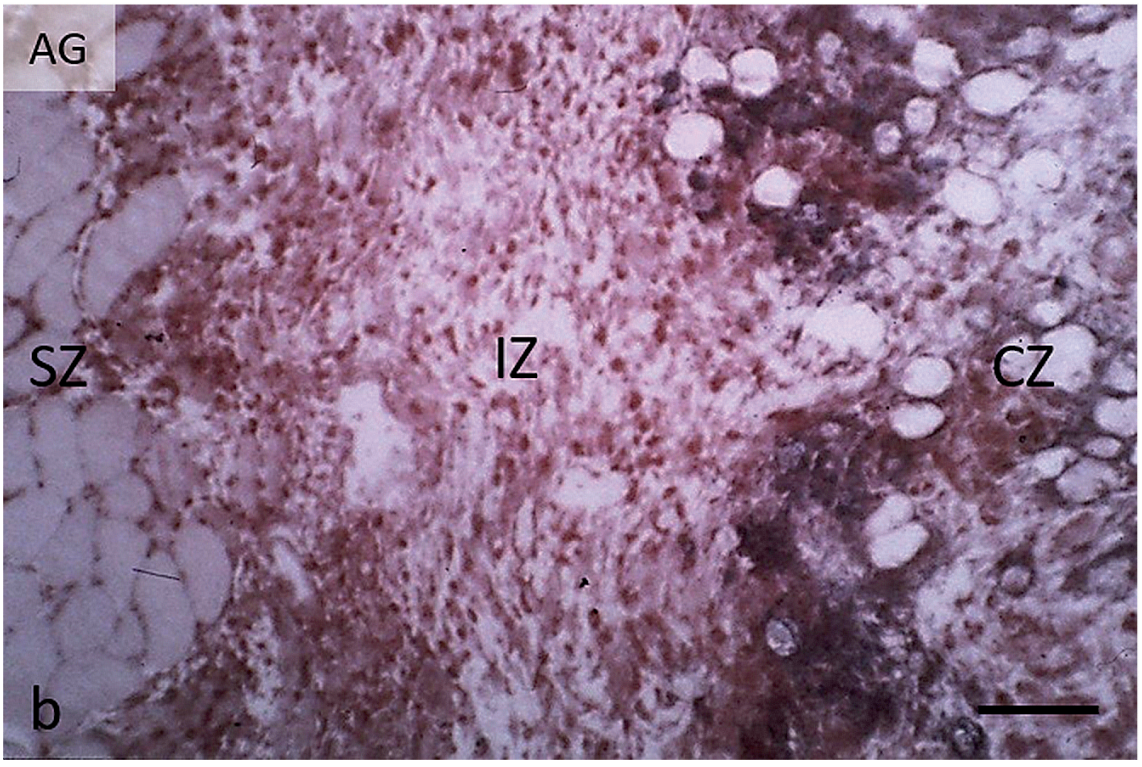

Fig. 2. Zoning of the implantation site.
a. Schematic representation of cross-sections of the AT muscle showing the three zones observed 7 days in MI group (left) and AG group (right).
b. Cross section of a muscle corresponding to the AG group, in which the presence of macrophages is highlighted by their acid phosphatase activity mainly in IZ. SZ: surviving zone; IZ: intermediate zone; CZ: central zone. Scale bar: 120 μm.

used depending on whether or not the data failed the normality test. Differences were considered significant with p values <0.05.

Results

At 7 days

Within this period, three different zones were evidenced in the cross section of the muscles of the MI, FAG, and AG rats: central zone (CZ), intermediate zone (IZ), and surviving zone (SZ) (Fig. 2a). The CZ of the muscles of the MI group was occupied by degenerated and necrotic muscle fibers (data not shown). In the FAG (data not shown) and AG groups, the implanted adipose tissue was surrounded by a significant number of inflammatory cells with high acid phosphatase activity (Fig. 2b). In the proximity of the SZ, the IZ contained regenerative muscle fibers of varying density (MI: 95%; AG: 49%; and FAG: 4.4%) and histological (Fig. 3a-c), histochemical (Fig. 4a-d) and immunohistochemical (Fig. 5a-d) staining behaviors among the different groups. Whereas in the MI group the staining for desmin and laminin revealed a highly arranged pattern of regeneration and persistence of the basal laminas (Fig. 5a,b) respectively, mononuclear desmin-positive cells interspersed between the implanted tissue and an absence of basal laminas was observed in the AG group (Fig. 5c,d).

At 14 days

In the MI group, the IZ was seen to be occupied by regenerative muscle fibers of larger size, with fewer basophilia (Fig. 6a), and which already showed differentiated fiber types with the NADH-tr histochemical technique (Fig. 6b). However, in the AG group, the fibers were found to be heterogeneous in

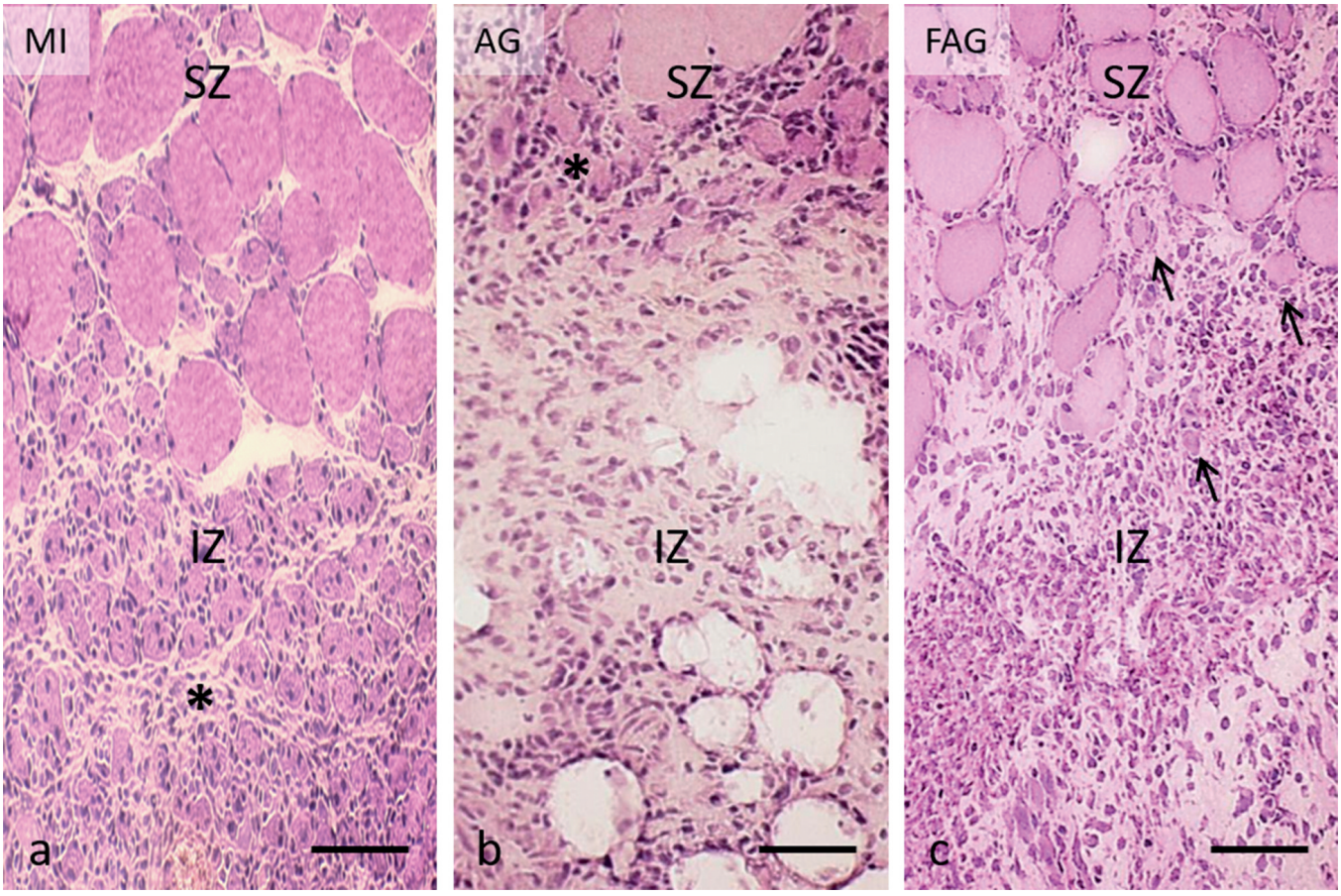

Fig. 3. Representative micrographs of the histology of the intermediate zone (IZ). **a.** MI group: the IZ is occupied by a dense mass of small, basophilic, regenerative muscle fibers with central nuclei (asterisk). **b.** AG group: the density of the regenerative fibers is much lower, and the fibers are located in the vicinity of the SZ (asterisk) while the rest of the IZ is occupied by inflammatory and adipose cells. **c.** FAG group: the IZ is invaded by inflammatory cells, and only a few regenerative muscle fibers interspersed between the apparently normal SZ muscle fibers are observed (arrows). H&E. Scale bars: 50 μm.

terms of their degree of maturity (size variations and intrasarcoplasmic distribution of the basophilia) (Fig. 6d). Many of them had features indicative of abnormal regeneration (nuclear accumulations, internal disorientation, and cracking) (Fig. 6d) or cytoarchitectural changes of the targetoid type (indicative of denervation-reinnervation) in the form of central areas of strong oxidative activity (Fig. 6e). The most noteworthy observation was the presence of myotubes either isolated or forming small groups scattered in the IZ and the CZ. These structures had variable histological features indicative that they were at different stages of maturity and variable desmin staining patterns, with the presence of cytoarchitectural alterations being the most noteworthy finding, contrasting with MI group (Fig. 6c,f). In the FAG group, the regenerative fibers appeared to be suffering degenerative changes and were surrounded by an important inflammatory response (Fig. 6 g-i).

In AG group the ATPase stain revealed the existence of vascularization in the three zones (Fig. 7a). This indicated that the implanted adipose tissue appeared to be integrated by revascularization from the SZ. By contrast, in the FAG group, the implanted adipose tissue showed signs of destruction by freezing and was isolated by a band of inflammatory cells (Fig. 7b,c). In this group the regenerative response at the edge of the lesion was residual.

At 21 days

In the MI group, the injury site was recognized by the presence of regenerated muscle fibers with internal nuclei and discretely variable sizes. The differentiation

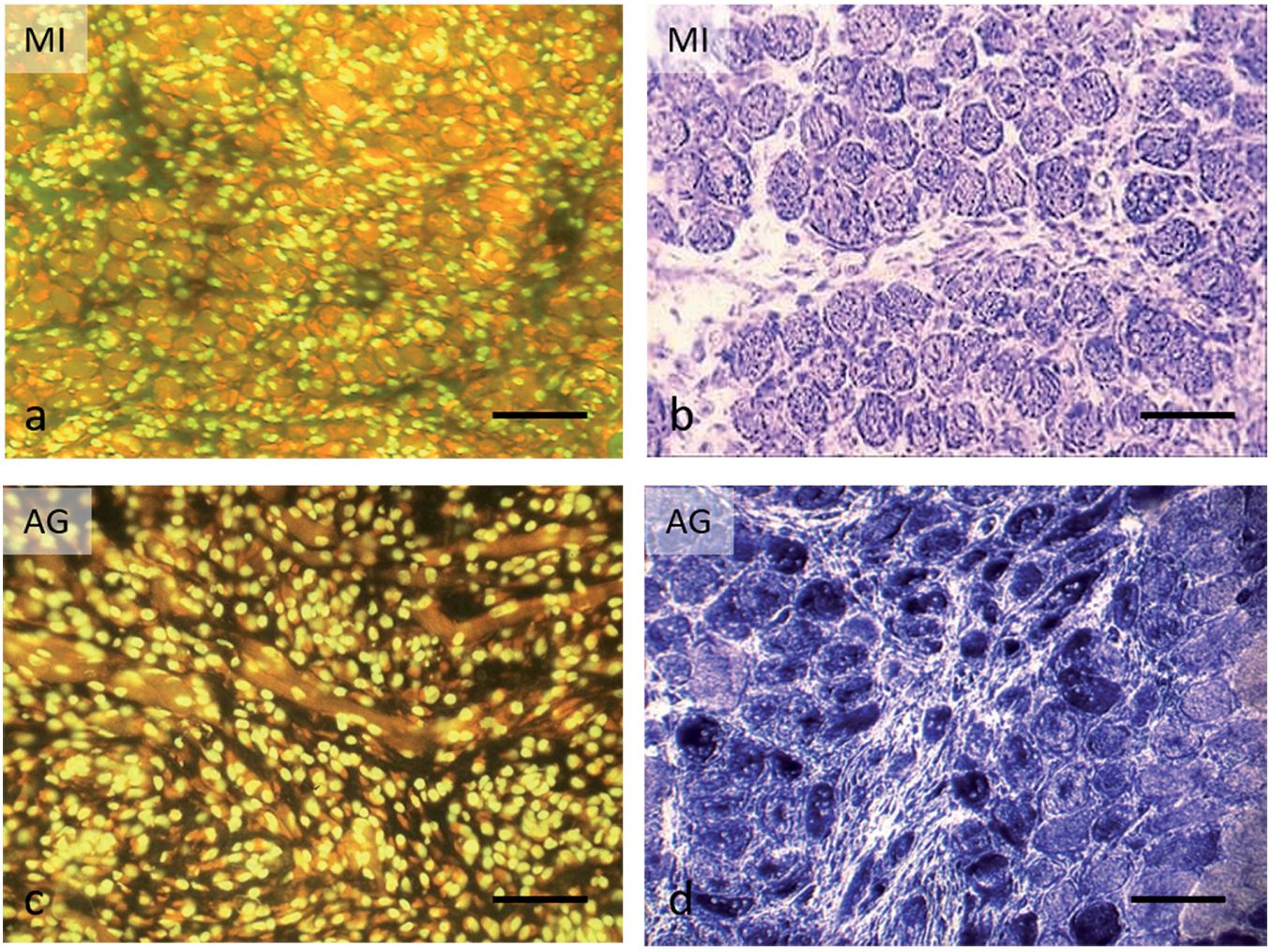

Fig. 4. Comparison of the histochemical features at 7 days between the regenerative fibers of MI, and AG groups. MI group: cross-sections revealing regenerative muscle fibers with orange fluorescence **(a)** and an uniform reticular pattern of high oxidative activity **(b)**. AG group: cross sections of regenerative muscle fibers with low orange fluorescence **(c)** and heterogeneous staining of oxidative activity without a reticular pattern **(d)**. AO [a, c] NADH-tr [b, d]. Scale bars: a, c, d, 50 μm; b, 20 μm.

in fiber types was already evident at this time, and no prominent features were detected in the immunohistochemical analysis (Fig. 8a). In the AG group, the IZ and CZ were still evident. The presence of muscle fibers with internal nuclei, markedly variable sizes, and disorientation were the most noteworthy findings in this group (Fig. 8b). Some fascicles were also seen to contain ring fibers (Fig. 8c). This altered pattern was very evident with the staining for desmin (Fig. 8d). MyoD-positive nuclei were seen both in the regenerative fibers of the IZ and between the adipocytes of the central zone in AG group (Fig. 9a,b). On the contrary, in the FAG group, positive nuclei were observed for MyoD neither at the level of the scarce regenerative fibers nor between the remains of the adipose tissue (Fig. 9c,d).

At 28 days

In general, the observations made within this timeframe were similar to those made at 21 days. In the MI group, the muscle fibers were completely regenerated and did not exhibit abnormalities when using the histochemical and immunohistochemical techniques, with the most remarkable finding being the presence of internal nuclei (data not shown). On the other hand, an outstanding variability in the size of the muscle fibers and the disorientation was observed in the AG group. The behavior of these fibers with the histochemical and immunohistochemical techniques was similar to that observed during the previous period, and the presence of cytoarchitectural abnormalities was confirmed (Fig. 10a,b). In the FAG group, the area of implantation was occupied by connective tissue and there was a persistent inflammatory response (Fig. 10c). Between this area and the SZ, occasional small muscle fibers (probably regenerative fibers that would have remained atrophic) are seen (Fig. 10c,d).

At 60 days

At this time, the histoarchitectural muscle features varied significantly among the different groups (Fig.

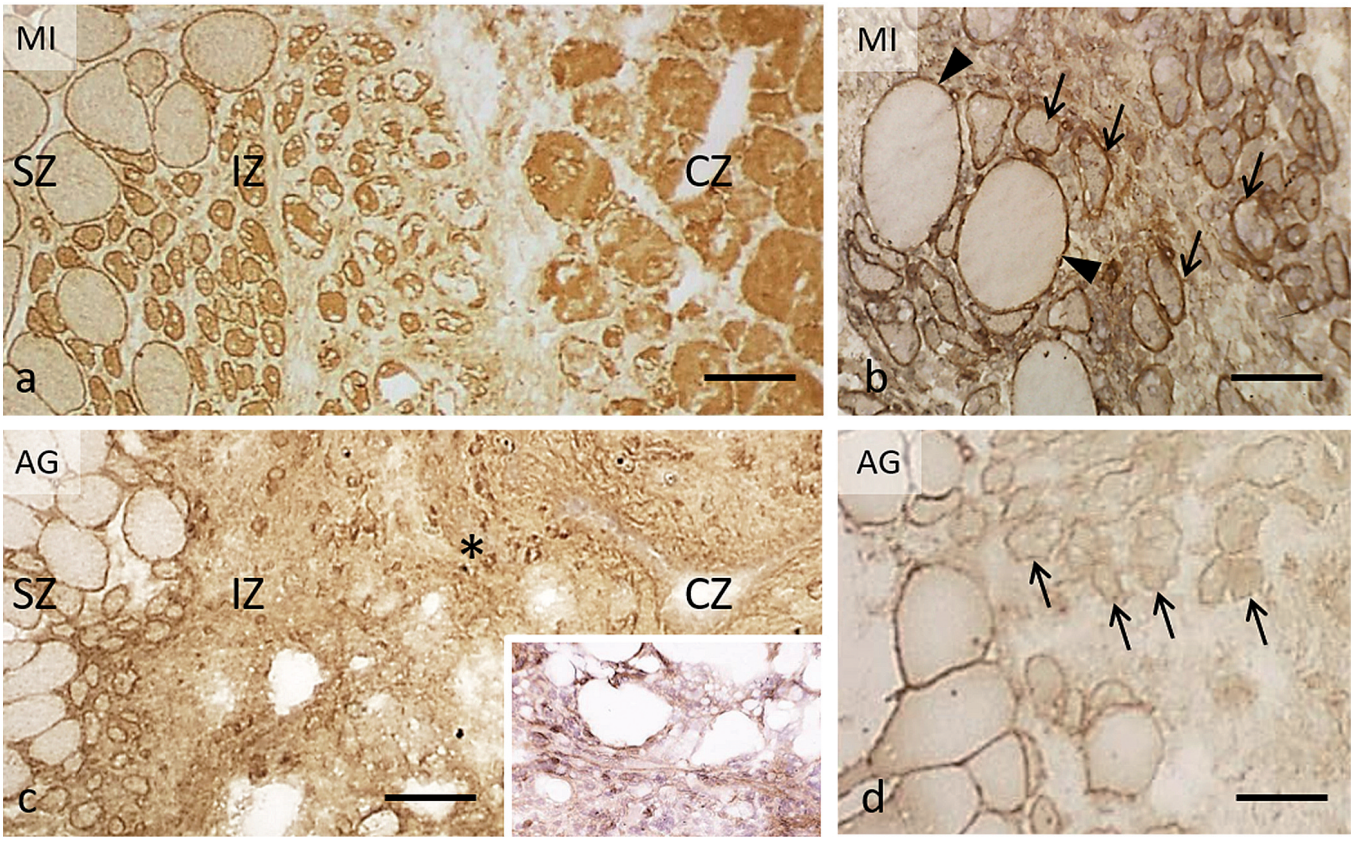

Fig. 5. Immunohistochemical analysis of desmin and laminin in MI, and AG groups. MI group: cross-sections revealing regenerative muscle fibers with strong and homogeneous staining for desmin arranged in an orderly manner in the intermediate zone **(a)** and basal laminas marked with anti-laminin in normal (arrowheads) and regenerative muscle fibers (arrows) **(b)**. AG group: cross-sections of regenerative muscle fibers with low intrasarcoplasmic anti-desmin staining **(c)**, marked along the periphery, and abundant desmin-positive mononuclear cells (asterisk) arranged in a disorderly manner in the intermediate zone next to adipose cells. Insert: observe how the small desmin-positive cells surround the adipocytes. **d.** Absence of basal laminas with anti-laminin in regenerative muscle fibers (arrows). Anti-desmin [a, c, insert]; anti-laminin [b, d]. Scale bars: a, c, 100 μm; b, d, 50 μm.

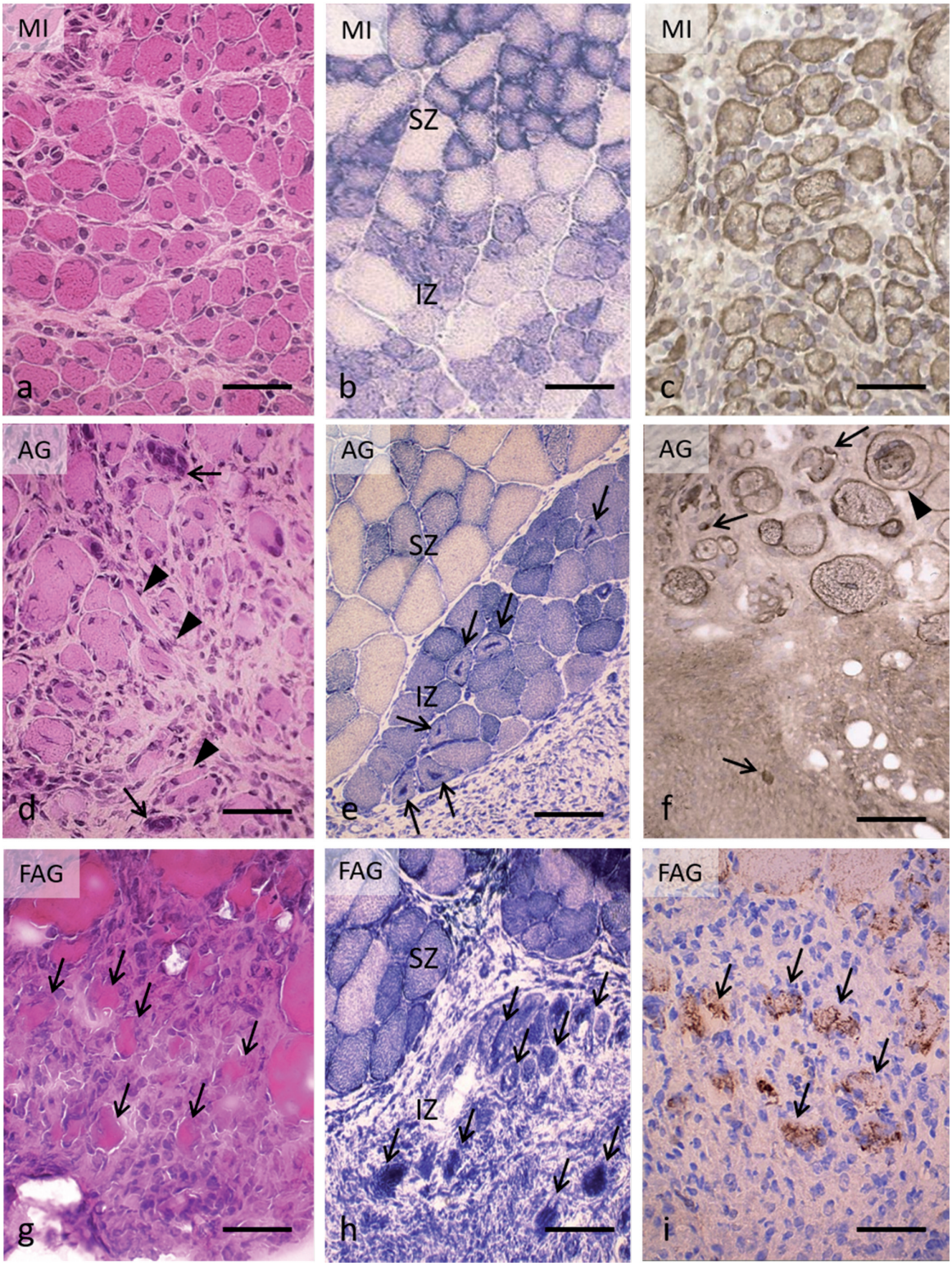

Fig. 6. Microscopic characteristics at 14 days of the regenerative muscle fibers located in the IZ of MI, AG, and FAG groups. MI group: regenerative muscle fibers with moderate basophilia and a homogeneous size **(a)**, differentiation in histochemical types **(b)**, and a homogeneous reticular staining pattern for desmin **(c)**. AG group: regenerative muscle fibers of variable size and morphology **(d)**, some disoriented (arrowheads) and others with accumulations of nuclei (arrows); **(e)** there is no clear muscle fiber typing, and several have central areas of high oxidative activity (arrows); **(f)** muscle fibers with heterogeneous staining patterns, including a snake-coil fiber (arrowhead); we also observed desmin-positive mononuclear cells (arrows). FAG group: **(g)** small regenerative fibers of degenerative aspect showing irregular morphology, acidophilia and without central nuclei (arrows), surrounded by inflammatory cells. **(h)** muscle fibers with abnormal patterns of oxidative staining (arrows). **(i)** several fibers showing disruption of desmin immunolabelling (arrows) H&E [a, d, g]; NADH-tr [b, e, h]; anti-desmin [c, f, i]. Scale bars: a, c, d, f, g, i, 50 μm; b, e, h, 100 μm.

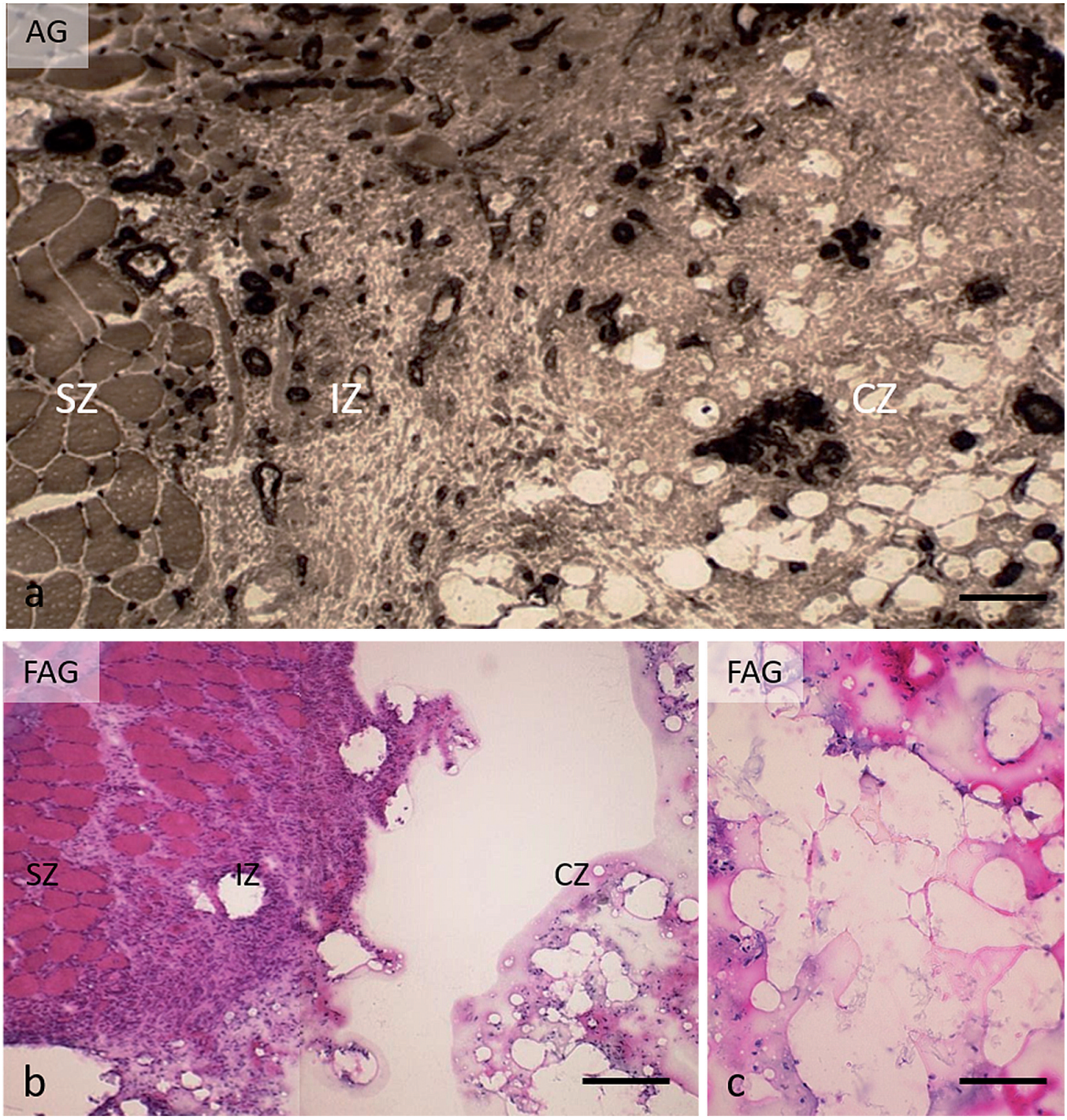

Fig. 7. Representative micrographs of the vascular integration of the adipose tissue implanted in the host muscle in the AG group and of non-integration in the FAG group. AG group: image showing visible vascularization in the three zones at low magnification **(a)**. Blood vessels are stained black. FAG group: cross section in which the three zones are observed **(b)**. The IZ is occupied by a large inflammatory reaction and CZ frozen adipose tissue is retracted. Detail of the degenerative aspect of frozen adipose tissue **(c)**. The adipocytes are broken and the nuclei are pyknotic. ATPase, pH 9.4 [a]; H&E [b, c]. Scale bars: a, 100 μm; b, c, 50 μm.

11a-d), a finding that was confirmed by histomorphometric analysis. There were significant differences in the percentage of area occupied by connective tissue among all the groups: while in a normal muscle it represented 2.89±0.25%, in the MI group it was 5.80±0.52%, 19.57±3.47% in the AG group and 59.50±1.47% in the FAG group (Fig. 12). Therefore it was evident that in the AG group, 80% of the implanted autologous adipose tissue was replaced by muscle tissue. While the presence of fibers with internal nuclei was the most common characteristic in the three experimental groups, the main histological features of the newly formed muscle fibers in AG group were disorientation and variability in their sizes (Table 1). While in the MI group the regenerated muscle fibers had recovered their organization in fascicles similarly a normal muscle, this recovery did not occur in the AG group (Fig. 11).

Discussion

Our observations prove that an area of VML can be reconstructed by means of the implantation of autologous adipose tissue, as this tissue is progressively replaced by new muscle tissue. This is due to the generation of new muscle fibers in the surviving area surrounding the implant, as well as of other fibers seemingly originating within the thickness of the adipose tissue. However, in our study, the formed neo-muscle presented structural differences not only with respect to

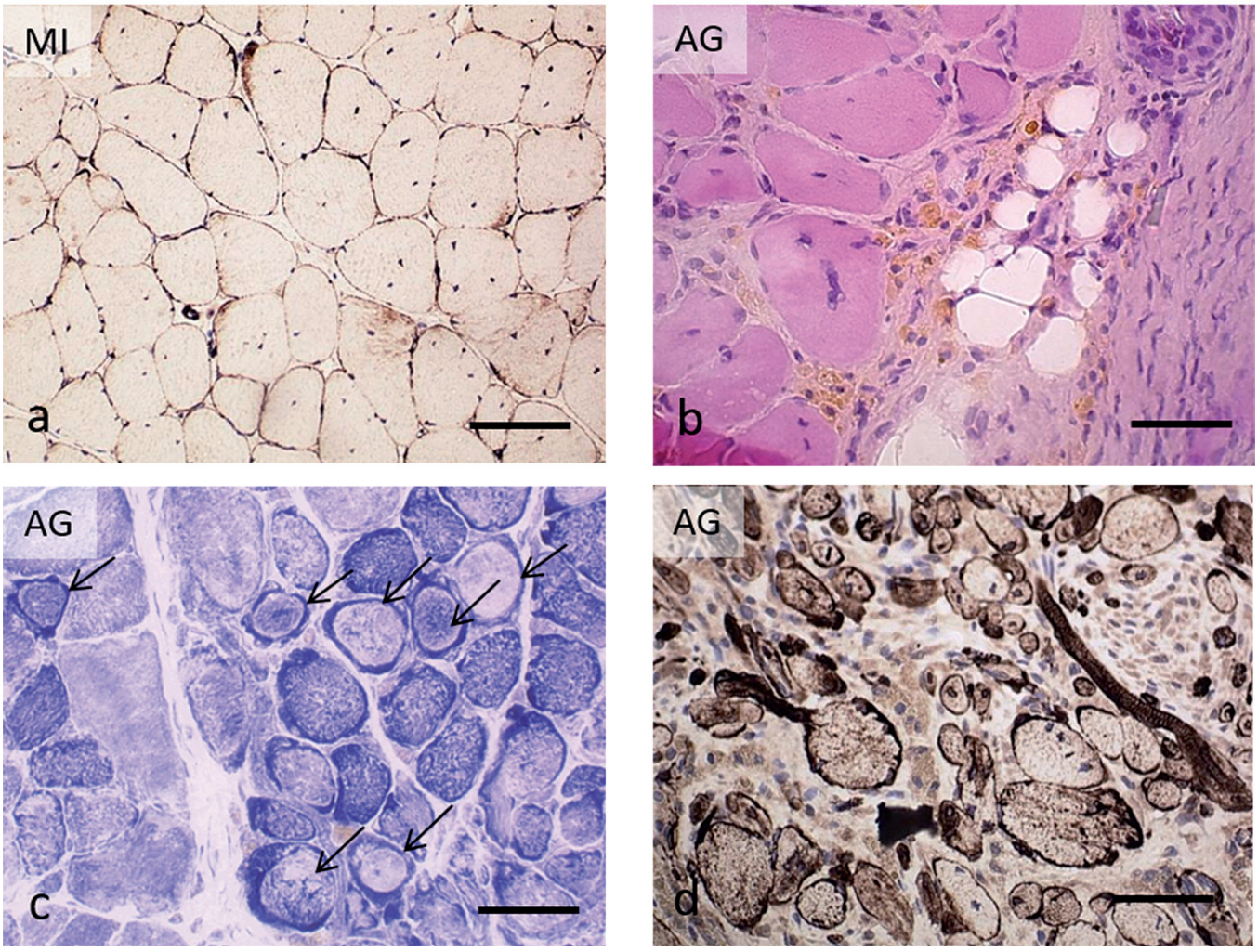

Fig. 8. Microscopic features of regenerative muscle fibers at 21 days in groups MI and AG. MI group: regenerated muscle fibers with internal nuclei and no expression of desmin except at a subsarcolemmal level **(a)**. AG group: Muscle fibers of variable size, with internal nuclei next to a focus of fibrosis with adipocytes and macrophages with hemosiderin **(b)**. **c.** The fibers show differentiation in types, with some corresponding to ring fibers (arrows). **d.** Muscle fibers with great variability in size, desmin expression, and orientation. Desmin [a, d]; H&E [b]; NADH-tr [c]. Scale bars: a, 50 μm; b-d, 100 μm.

the normal skeletal muscle, but also to the muscle formed by means of a normal regeneration process such as in the case of the muscles of the MI group. The differences were already evident at 7 days, with a delay in the density and the degree of maturity of the regenerative fibers. At more advanced phases, these differences were reflected by the variability in the size of the regenerative fibers, their disorientation, their cytoarchitectural abnormalities, and a certain degree of fibrosis.

Our study confirmed the ability of the muscle tissue to participate in the reconstruction of an area of VML

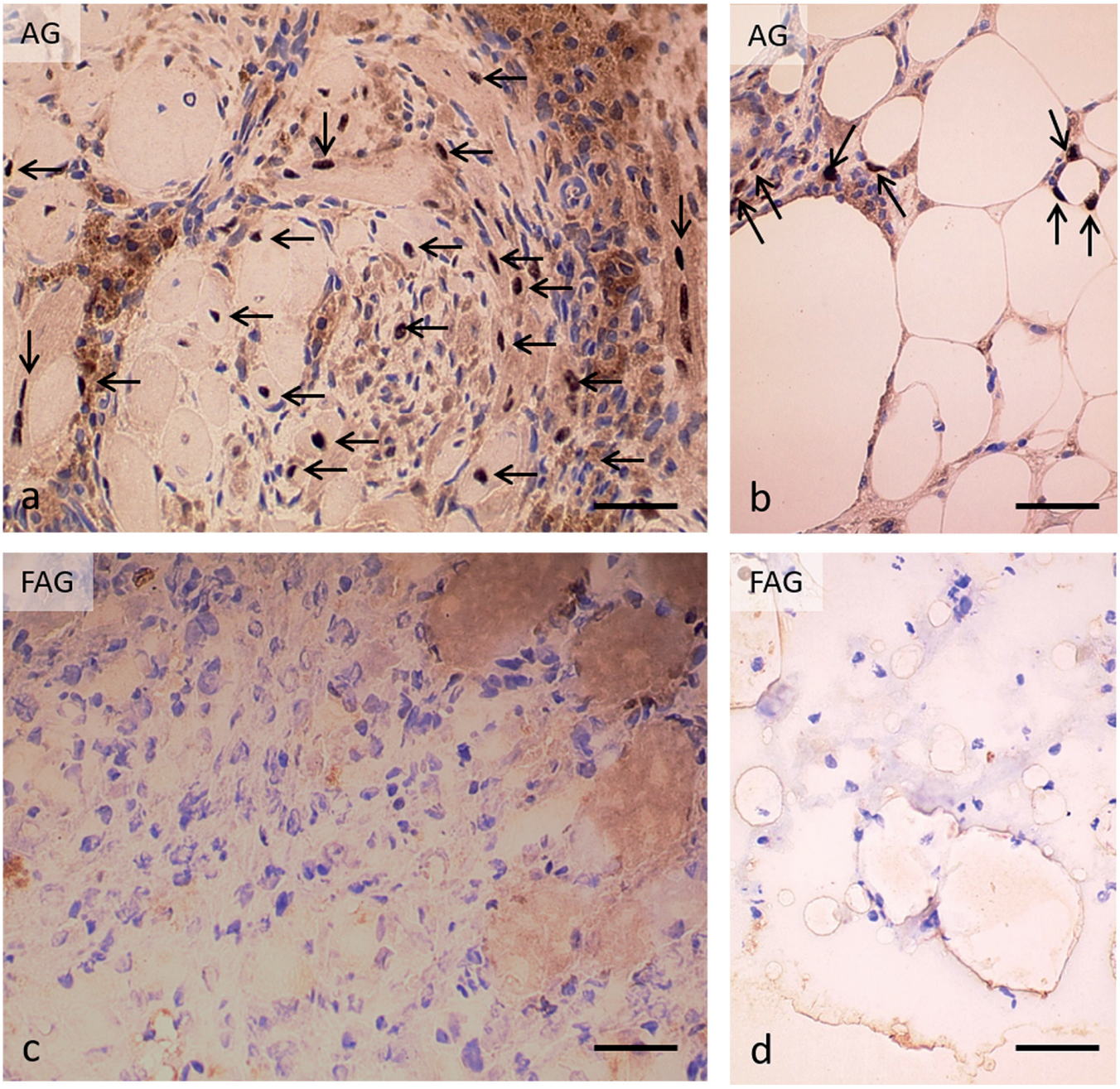

Fig. 9. Immunolocalization of MyoD nuclei in AG and FAG groups. AG group: Intermediate zone: cross section revealing oriented and disoriented regenerative muscle fibers containing MyoD-positive nuclei (arrows) **(a)**. Central zone: MyoD-positive nuclei (arrows) dispersed between adipocytes (arrows) **(b)**. FAG group: Intermediate zone: No labeled nuclei are observed with MyoD **(c)**. Central zone: Adipose cells are broken and not MyoD labeled nuclei are observed **(d)**. Scale bars: 30 μm.

from the edges of the severed muscles, as the regenerative response of a muscle originating in the surviving zones is very powerful. In experimental models involving orthotopic transplantations (Carlson, 2007), the intramuscular injection of myotoxins (Vignaud et al., 2005; Jiménez-Díaz et al., 2012), and crush injuries (Takeuchi et al., 2014) in which the central zone of the muscle degenerates, a characteristic pattern of degeneration and centripetal regeneration in which myotubes or regenerative muscle fibers grew from the surviving areas and managed to regenerate the practical entirety of the injury within 30 days was initiated. While in the MI group the regeneration was seen to be fast and efficient, with an almost complete reconstitution of the muscular histoarchitecture and only some remaining internalized nuclei, in the AG group the histology of the neo-muscle differed from that seen following the normal regenerative process of the MI group throughout all the analyzed time periods.

Although myotubes can penetrate the thickness of the implanted adipose tissue from the edges of the muscle defect (Satoh et al., 1992), it is clear that they do so without having a scaffold basal lamina or satellite cells acting as a source of myoblasts in the injured area (Corona and Greising, 2016). This may partly justify the fact that the new muscle fibers in the AG group showed clear differences in comparison with the regenerative muscle fibers of the MI group, as these elements

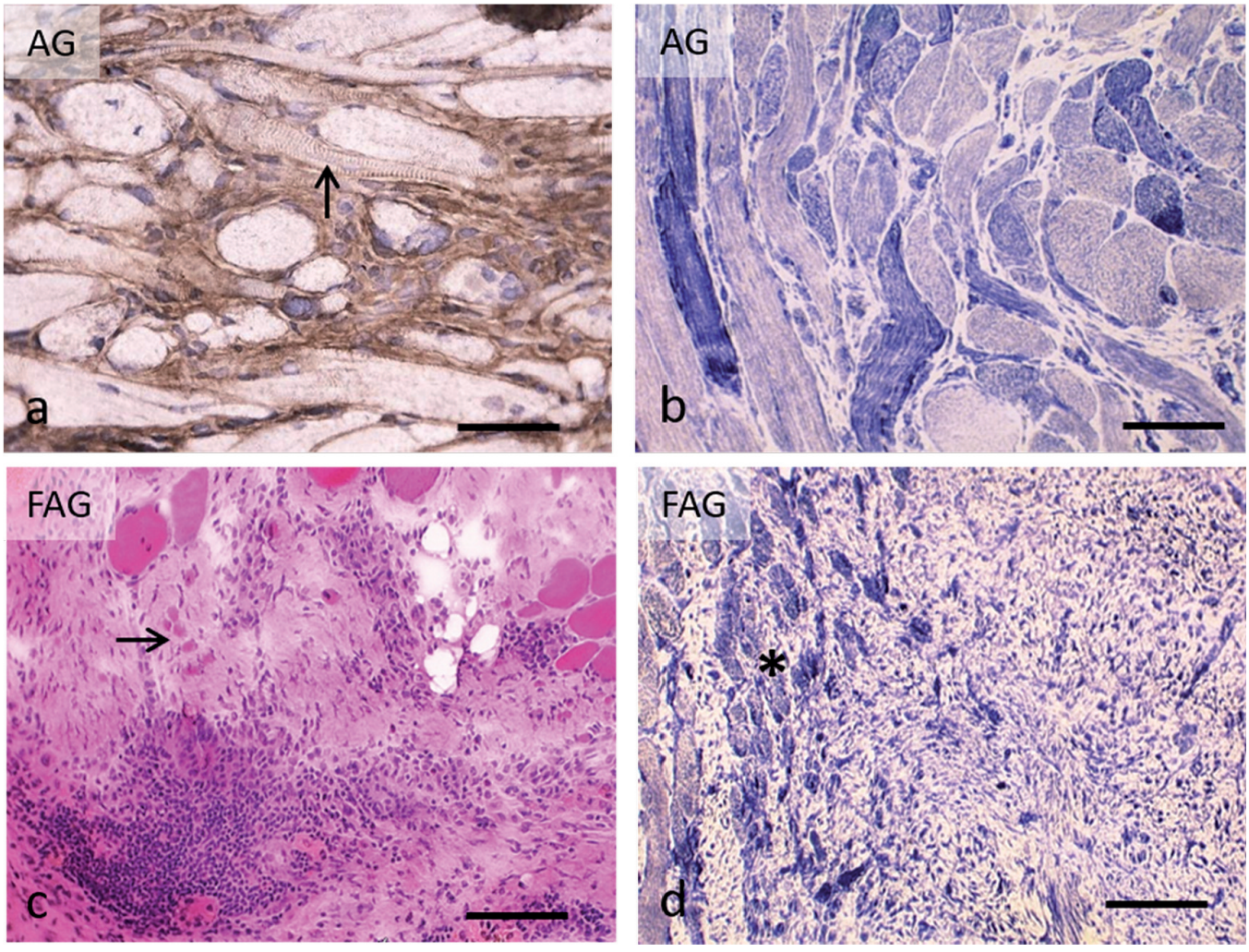

Fig. 10. Microscopic features of regenerative muscle fibers at 28 days in AG and FAG groups. AG group: **a.** Muscle fibers of variable size and morphology, completely disoriented. In some fibers, the transversal striations are evident (arrow). **b.** Despite their abnormal histoarchitecture, the muscle fibers show differentiation in histochemical fiber types. FAG group: **c.** Foci of inflammatory cells and small fibers isolated (arrow) in the thickness of the connective tissue. **d.** To the left of the image, the limit of the surviving area is observed, together with small fibers without differentiation of histochemical types (asterisk). On the right, the entire area of the implant is characterized by the absence of muscle fibers. Anti-desmin [a]; NADH-tr [b, d]; H&E [c]. Scale bars: a, b, 50 μm; c, d, 100 μm.

remained more or less intact in the MI group (Biérinx and Sebille, 2008). The basal laminas play a decisive role in promoting the growth and orientation of the regenerative muscle fibers, nerves, and blood vessels (Sanes, 2003), as well as preventing fibroblasts and collagen from interfering with the continuity of the fiber (Mann et al., 2011). The difference between the histological features of the neo-muscle formed in the AG group and those of the muscle formed by means of a normal regenerative process in the MI group may be explained by the importance of the reintegrative factors (revascularization, reinnervation, and mechanical reintegration) in the muscle regeneration process (Carlson, 2007; Turner and Badylak, 2012). Evidently, in our case the induced deficit in the muscle volume resulted in a disruption of the supply of vascular and nervous structures, and the neoformation of muscle tissue in the thickness of the adipose tissue was not subjected to tensile forces owing to the lack of tendinous connections. Based on the type of abnormalities identified in our study, we believe that the low-tension environment in which the new muscle fibers grew played an essential role in determining the histological characteristics of the neo-muscle. Previous studies have demonstrated that when regenerative or repair muscle fibers are formed in a low-tension environment, cytoarchitectural changes related to myofibrillar disorientation occur, such as the formation of ring fibers,

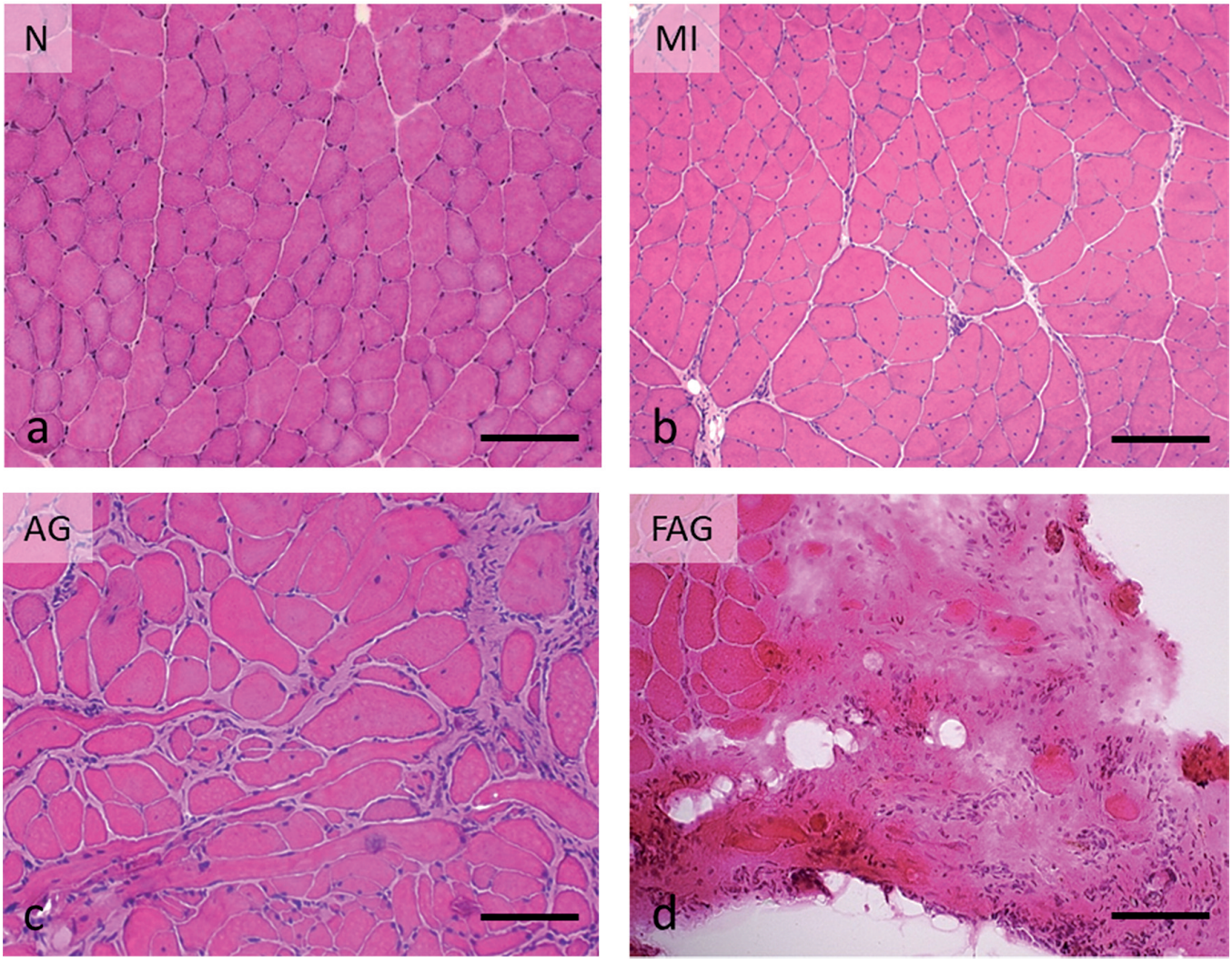

Fig. 11. Representative micrographs of muscle histoarchitecture at 60 days of the N, MI, AG and FAG groups. Cross sections of muscles corresponding to: **a.** Normal group: normal muscle fibers, with polygonal morphology and peripheral nuclei, arranged in fascicles. **b.** MI group: regenerated muscle fibers, with polygonal morphology and internal nuclei, arranged in fascicles. **c.** AG group: muscle fibers of variable morphology and size, disoriented, and some with internal nuclei. Note the endomysial fibrosis and lack of organization in fascicles. **d.** FAG group: the area is occupied by enough fibrous tissue, some inflammatory cells, and isolated muscle fibers. H&E. Scale bars: 100 μm.

trabeculated fibers, or snake-coil fibers (Peña et al., 2001, 2005), in addition to the enhancement of muscle fibrosis (Luque et al., 2002). Split fibers have also been associated with failures or delays in the fusion of the regenerative myotubes (Eriksson et al., 2006) and branched fibers observed in the ectopic formation of muscle following the implantation of myoblasts below the skin (Irintchev et al., 1998).

Another noteworthy finding of our study was the disorientation of the muscle fibers, which reached a prevalence of 24% in the AG group in comparison with only 0.8% in the MI group. This occurs in the minced muscle implantation model, in which the absence of tendon connections results in the random arrangement of muscle fibers (Corona et al., 2013, 2017; Ward et al., 2016). The parallel orientation of the muscle fibers is a fundamental step affected by mechanical stimuli, regardless of the neural, hormonal, or electrical influences (Collinsworth et al., 2000; Kuthe and Uddanwadiker, 2016). Given that the basal laminas act as scaffolds for the alignment of the new fibers, their absence must have been a determining factor in the disorientation and the abnormalities seen in the new muscle fibers.

Our study also highlighted the difficulties encountered by the new fibers in being innervated. Thus, the presence of fibers with central spots and clusters of fiber types is related to innervation/reinnervation processes, whereas the existence of atrophic fibers (some with nuclei clumping) in the thickness of the foci of fibrosis confirms the failed innervation of the new fibers. Although the myotubes and regenerative fibers are formed in an aneural environment, both maturation and growth fail in the absence of innervation (Noah et al., 2002). It is clear that fibrosis is directly involved in the failure of innervation by creating physical barriers that prevent the nerve fibers from coming into contact with the muscle fibers (Huard and Fu, 2002; Järvinen et al., 2007; Turner and Badylak, 2012).

Although the great regenerative capacity of skeletal muscle is ineffective in spontaneously recovering lesions due to VML (Sicari et al., 2012) our results in the AG group reached an important neoformation of muscle. In our study, although the percentage of fibrotic area in the AG group (20%) was significant in comparison with that of the normal group (3%) and the MI group (6%), the formation of muscle in the defect indicated that adipose tissue favored the growth of new muscle fibers considering that the percentage of fibrosis in the FAG group was close to 60%. This can be explained by the fact that the implanted adipose tissue was frozen or not. The presence in the implanted adipose tissue of MyoD $^{+}$ nuclei as well as myotubes and mononuclear cells positive for desmin in the AG group, would be indicative that cells located in the adipose tissue would have undergone myogenic differentiation. In contrast, the absence of myogenic markers in the FAG group confirmed that a previous freezing treatment would destroy the cells and, therefore, could not contribute to the formation of new muscle fibers, favouring fibrosis. The expression of these markers allows the identification of precursors of myogenic cells in the processes of neoformation and muscle regeneration (Agüera et al., 2019).

Stromal cells derived from adipose tissue-derived stromal cells (ATDSCs) have the potential to differentiate into cells and tissues of mesodermal origin (Schäffler and Büchler, 2007; Lin et al., 2010; Gentile and Cervelli, 2018). Although we cannot determine exactly which types of implanted adipose tissue cells experienced myogenic differentiation, it has been observed that the transplanted ADSCs were involved in the muscle regeneration process (Bacou et al., 2004). Di Rocco et al. (2006) found that cells of the stromal-vascular fraction of adipose tissue (AT-SVF) can differentiate into skeletal muscle by adopting a myogenic phenotype when they are cultivated together

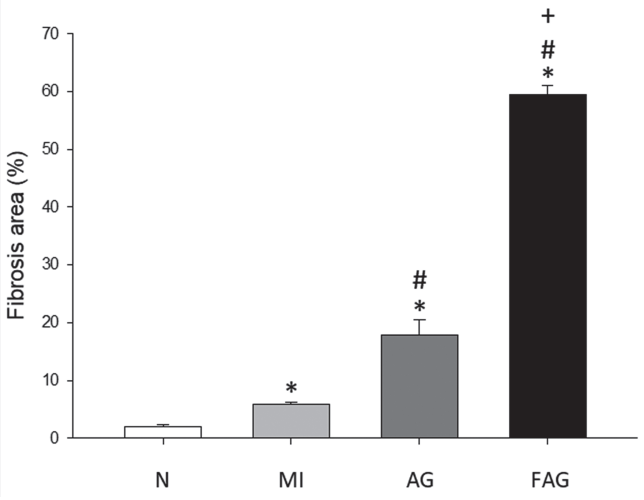

Fig. 12. Comparison of the fibrotic area between the different groups at 60 days. * p<0.05 vs normal group; # p<0.05 vs myotoxin-injured group; + p<0.05 vs adipose graft. N: normal group; MI: myotoxic injury group; AG: adipose graft group; FAG: frozen adipose graft group.

Table 1. Histomorphometric parameters of muscle fibers at 60 days.

Group	muscle fibers cross-sectional area	muscle fibers number	muscle fibers with internal nuclei	disoriented muscle fibers
N	3400.6±184.4	14.8±0.7	4.2±1.6	0.01±0.01
MI	3514.8±157.8	14.8±0.4	68.8±3.4*	0.87±0.07*
AG	2385.0±541.0*†	16.8±1.7	62.3±5.1*	23.9±3.0*†
FAG	463.6±411.0*†§	6.7±0.4*†§	70.2±9.0*	0.34±0.5*†§

All values are expressed as mean ± SEM. * P<0.05 vs N group; † P<0.05 vs MI group; § P<0.05 vs AG group. N, normal group; MI, myotoxic injury group; AG, adipose graft group; FAG, frozen adipose graft group.

with primary myoblasts. In addition, an *in vivo* study using an experimental ischemia model proved that these cells of the AT-SVF fraction form new muscle fibers, and another model using mdx mice showed that they significantly restore dystrophin expression. Finally, these authors indicated that factors secreted by the myogenic cells in differentiation are sufficient for a subpopulation of AT-SVF cells to express muscle-specific proteins. There is evidence that mesenchymal cells derived from adipose tissue would be the best option, compared to those derived from bone marrow or synovial membrane, to contribute to muscle regeneration in the treatment of some myopathies with mesenchymal stem cells (de la Garza Rodea et al., 2012).

The intimate mechanism of this myogenic differentiation is most likely related to the tissue microenvironment generated in the skeletal muscle and the intercellular relationships. The microenvironment of each tissue affects the differentiation potential of both specific and non-specific stem cells (Peng and Huard, 2004). The regenerative capacity of skeletal muscle and the response of the satellite cells to the injury are significantly determined by changes in various factors within the local tissue environment (Jejurikar and Kuzon, 2003) that constitute an important source of signals recruiting cells towards the myogenesis (De Angelis et al., 1999). Salvatori et al. (1995) proved that stem cells from different organs differentiate into the myogenic line when cultivated together with myogenic cells. This also occurs *in vivo*, in which case a close cell-cell relationship, but not necessarily cell fusion, is required. It has recently been shown that the co-culture of myoblasts in the presence of neural cells stimulates the differentiation and formation of myotubes, their alignment, length and covered area (Ostrovidov et al., 2017). Consequently, we might think that the growth of new fibers could be favored by the adipose tissue itself due to the creation of a favorable pro-myogenic environment. Several cell types secrete microvesicles and/or exosomes that have functional and phenotypic effects on other cells. In this sense, it is very probable that the exosomes secreted by ADSCs (Wong et al., 2019) as well as by the satellite cells (Spinazzola and Gussoni, 2017) residing in the host muscle are involved in the myogenic response generated after adipose tissue implantation. Furthermore, it is interesting to note that exosomes are also secreted during the differentiation of human myoblasts, which raises its utility as an agent for muscle regeneration (Choi et al., 2016). Interestingly ADSCs therapy accelerates functional recovery and increases the number of myofibers in regeneration, but does not detect ADSCs myogenic differentiation, suggesting that these cells act through direct cellular-paracrine mechanisms by secretory factors involved in the regeneration of skeletal muscle (Gorecka et al., 2018). However, our immunohistochemical observations showed that cells residing in the adipose tissue underwent myogenic differentiation. In our opinion, this contradiction can be explained by the fact that the behavior may be different when isolated ADSCs are transplanted, which, as in the present study, is transplanted adipose tissue.

In our study, the neoformation of muscle fibers in the AG group was accompanied by important vascular neoformation. It is a well-known fact that the promotion of angiogenesis is one of the key factors required to stimulate the repair process in cases of VML (Turner and Badylak, 2012), although the essential role of the blood vessels, the immune and inflammatory cells, the circulating progenitors, and the resident cells in the regeneration/repair process is not known exactly (Huard, 2019). Revascularization could have been favored by the adipose tissue itself, since stromal cells derived from adipose tissue have considerable pro-angiogenic potential (Schäffler and Büchler 2007). It is important to note that when stem cells derived from human adipose tissue are implanted in combination with bundles of fibrin microfiber in a murine model of VML, muscle reconstruction *in vivo* is very moderate (Gilbert-Honick et al., 2018). Since in our study adipose tissue was largely replaced by muscle tissue, we suggest that the use of autologous adipose tissue might be a better alternative to reconstruct the VML.

In conclusion, our results support the hypothesis that (at least from a morphological point of view), the transplantation of autologous adipose tissue favors the reconstruction process in cases of volumetric loss of skeletal muscle. Although the neoformed muscle tissue in the area of VML had some structurally abnormal features, we believe that the combination of appropriate rehabilitation strategies could aid in achieving histological and functional normality to a greater degree (Gentile et al., 2014; Greising et al., 2016). It has been found that after implantation of bioconstructs in a VML in mice, exercise improves reinnervation of neofibers, increases vascularization and reduces fibrosis (Quarta et al., 2017). This is important since several of the histological abnormalities seen in our study could be reduced. Although different scaffolds are being used for the regeneration of volumetric losses in skeletal muscle injuries (Grasman et al., 2015; Sicari et al., 2015), this model could be useful to explore other possibilities available in muscle reconstruction. However, further research is needed to clarify the intimate mechanisms of the myogenic contribution of the adipose tissue to this process, as well as the development of therapeutic strategies leading to the restoration of the normal histoarchitecture of the skeletal muscle.

Acknowledgements. We are grateful to Mr. Antonio Agüera for all technical support and assistance.

References

Agüera E., Castilla S., Luque E., Jimena I., Ruz-Caracuel I, Leiva-Cepas F. and Peña J. (2019). Denervated muscle extract promotes recovery of muscle atrophy through activation of satellite cells. An

experimental study. J. Sport Health Sci. 8, 23-31.

Andersen D.C., Schrøder H.D. and Jensen G.H. (2008). Non-cultured adipose-derived CD45– side population cells are enriched for progenitors that give rise to myofibres *in vivo*. Exp. Cell Res. 314, 2951-2964.

Argentati C., Morena F., Bazzucchi M., Armentano I., Emiliani C. and Martino S. (2018). Adipose stem cell translational applications: from bench-to-bedside. Int. J. Mol. Sci. 9, 3475.

Aurora A., Roe J.L., Corona B.T. and Walters T.J. (2015). An acellular biologic scaffold does not regenerate appreciable *de novo* muscle tissue in rat models of volumetric muscle loss injury. Biomaterials 67, 393-407.

Bacou F., el Andalousi R.B., Daussin P.A., Micallef J.P., Levin J.M., Chammas M., Casteilla L., Reyne Y. and Nougues J. (2004). Trasplantation of adipose tissue-derived stromal cells increases mass and functional capacity of damaged skeletal muscle. Cell Trasplant. 13, 103-111.

Biérinx A.S. and Sebille A. (2008). Mouse sectioned muscle regenerates following auto-grafting with muscle fragments: A new muscle precursor cells transfer? Neurosci. Lett. 431, 211-214.

Carlson B.M. (2007). Reintegrative processes in regeneration. In: Principles of regenerative biology. Carlson B.M. (ed). Academic Press. pp 165-188.

Choi J.S., Yoon H.I., Lee K.S., Choi Y.C., Yang S.H., Kim I.S. and Cho Y.W. (2016). Exosomes from differentiating human skeletal muscle cells trigger myogenesis of stem cells and provide biochemical cues for skeletal muscle regeneration. J. Control. Release 28, 222 107-115.

Cholok D., Lee E., Lisiecki J., Agarwal S., Loder S., Ranganathan K., Qureshi A.T., Davis T.A. and Levi B. (2017). Traumatic muscle fibrosis: From pathway to prevention. J. Trauma Acute Care Surg. 82, 74-184.

Cittadella Vigodarzere G. and Mantero S. (2014). Skeletal muscle tissue engineering: strategies for volumetric constructs. Front. Physiol. 5, 362.

Collinsworth A.M., Torgan C.E., Nagda S.N., Rajaligam R.J., Graus W.E. and Truskey G.A. (2000). Orientation and length of mammalian skeletal myocytes in response to a unidirectional stretch. Cell Tissue Res. 302, 243-251.

Corona B.T. and Greising S.M. (2016). Challenges to acellular biological scaffold mediated skeletal muscle tissue regeneration. Biomaterials 104, 238-246.

Corona B.T., Garg K., Ward C.L., McDaniel J.S., Walters T.J. and Rathbone C.R. (2013). Autologous minced muscle grafts: a tissue engineering therapy for the volumetric loss of skeletal muscle. Am. J. Physiol. Cell Physiol. 305, C761-C775.

Corona B.T., Wenke J.C. and Ward C.L. (2016). Pathophysiology of volumetric muscle loss injury. Cells Tissues Organs 202, 180-188.

Corona B.T., Henderson B.E., Ward C.L. and Greising S.M. (2017). Contribution of minced muscle graft progenitor cells to muscle fiber formation after volumetric muscle loss injury in wild-type and immune deficient mice. Physiol. Rep. 5, e13249.

De Angelis L., Berghella L., Coletta M., Lattanzi L., Zanchi M., Cusella-De Angelis M.G., Ponzetto C. and Cossu G. (1999). Skeletal myogenic progenitors originating from embryonic dorsal aorta coexpress endotelial and myogenic markers and contribute to postnatal muscle growth and regeneration. J. Cell Biol. 147, 869-877.

de la Garza-Rodea A.S., van der Velde-van Dijke I., Boersma H., Gonçalves M.A., van Bekkum D.W., de Vries A.A. and Knaän-Shanzer S. (2012). Myogenic properties of human mesenchymal stem cells derived from three different sources. Cell Transplant. 21, 153-173.

Di Rocco G., Iachininoto M.G., Tritarelli A., Starino S., Sacheo A., Germani A., Crea F. and Capogrossi M.C. (2006). Myogenic potential of adipose-tissue-derived cells. J. Cell Sci. 119, 2945-2952.

Dubowitz V., Sewry C.A. and Oldfors A. (2013). Muscle biopsy. A practical approach. Fourth edition. Saunders Elsevier. Philadelphia. 2013.

Dunn A., Talovic M., Patel K., Patel A., Marcinczyk M. and Garg K. (2019). Biomaterial and stem cell-based strategies for skeletal muscle regeneration. J. Orthop. Res. 37, 1246-1262.

Ehrhardt J. and Morgan J. (2005). Regenerative capacity of skeletal muscle. Curr. Opin. Neurol. 18, 548-553.

Eriksson A., Lindström M., Carlsson L. and Thornell L.E. (2006). Hypertrophic muscle fibers with fissures in power-lifters; fiber splitting or defect regeneration. Histochem. Cell Biol. 126, 409-417.

Fuoco C., Petrilli L.L., Cannata S. and Gargioli C. (2016). Matrix scaffolding for stem cell guidance toward skeletal muscle tissue engineering. J. Orthop. Surg. Res. 11, e86.

Garg K., Corona B.T. and Walters T.J. (2014). Losartan administration reduces fibrosis but hinders functional recovery after volumetric muscle loss injury. J. Appl. Physiol. 25, 1120-1131.

Gentile P. and Cervelli V. (2018). Adipose-derived stromal vascular fraction cells and platelet-rich plasma: Basic and clinical implications for tissue engineering therapies in regenerative surgery. Methods Mol. Biol. 1773, 107-122.

Gentile N.E., Stearns K.M., Brown E.H.P., Rubin J.P., Boninger M.L., Dearth C.L., Ambrosio F. and Badylak S.F. (2014). Targeted rehabilitation after extracellular matrix scaffold transplantation for the treatment of volumetric muscle loss. Am. J. Phys. Med. Rehabil. 93 (Suppl), S79-S87.

Gilbert-Honick J., Ginn B., Zhang Y., Salhi S., Warner K.R., Mao H.Q. and Grayson W.L. (2018). Adipose-derived stem/stromal cells on electrospun fibrin microfiber bundles enable moderate muscle reconstruction in a volumetric muscle loss model. Cell Transplant. 27, 1644-1656.

Gomillion C.T. and Burg K.J.L. (2006). Stem cells and adipose tissue engineering. Biomaterials 27, 6052-6063.

Gorecka A., Salemi S., Haralampieva D., Moalli F., Stroka D., Candinas D., Eberli D. and Brügger L. (2018). Autologous transplantation of adipose-derived stem cells improves functional recovery of skeletal muscle without direct participation in new myofiber formation. Stem Cell Res. Ther. 9, 195.

Grasman J.M., Zayas M.J., Page R.L. and Pins G.D. (2015). Biomimetic scaffolds for regeneration of volumetric muscle loss in skeletal muscle injuries. Acta Biomater. 25, 2-15.

Greising S.M., Dearth C.L. and Corona B.T. (2016). Regenerative and rehabilitative medicine: a necessary synergy for functional recovery from volumetric muscle loss injury. Cells Tissues Organs 2016, 202 237-249.

Huard J. (2019). Stem cells, blood vessels, and angiogenesis as major determinants for musculoskeletal tissue repair. J. Orthop. Res. 37, 1212-122.

Huard Y., Li F. and Fu H. (2002). Muscle injuries and repair: Current trends in research. J. Bone Joint Surg. Am. 84-A, 822-832.

Irintchev A., Rosenblatt J.D., Cullen M.J., Zweyer M. and Wernig A. (1998). Ectopic skeletal muscles derived from myoblasts implanted

under the skin. J. Cell Sci. 111, 3287-3297.

Järvinen T.A.H., Järvinen T.L.N., Kääriäinen M., Äärimaa V., Vaittinen S., Kalimo H. and Järvinen M. (2007). Muscle injuries: optimising recovery. Best Pract. Res. Clin. Rheumatol. 21, 317-331.

Jejurikar S.S. and Kuzon W.M. Jr (2003). Satellite cell depletion in degenerative skeletal muscle. Apoptosis 8, 573-578.

Jiménez-Díaz F., Jimena I., Luque E., Mendizábal S., Bouffard A., Jiménez-Reina L. and Peña J. (2012). Experimental muscle injury: correlation between ultrasound and histological findings. Muscle Nerve 45, 705-712.

Kesireddy V. (2016). Evaluation of adipose-derived stem cells for tissue engineered muscle repair construct-mediated repair of a murine model of volumetric muscle loss injury. Int. J. Nanomedicine 11, 1461-1473.

Kuthe C.D. and Uddanwadiker R.V. (2016). Investigation of effect of fiber orientation on mechanical behavior of skeletal muscle. J. Appl. Biomater. Funct. Mater. 14, e154-162.

Kwee B.J. and Mooney D.J. (2017). Biomaterials for skeletal muscle tissue engineering. Curr. Opin. Biotechnol. 47, 16-22.

Lin C.S., Xin Z.C., Deng C.H., Ning H., Lin G. and Lue T.F. (2010). Defining adipose tissue-derived stem cells in tissue and in culture. Histol. Histopathol. 25, 807-815.

Liu J., Saul D., Böker K.O., Ernst J., Lehman W. and Schilling A.F. (2018). Current methods for skeletal muscle tissue repair and regeneration. Biomed. Res. Int. 2018, 1984879.

Long M.W. (2001). Stem cell plasticity: molding the future of tissue development and repair. Blood Cell. Mol. Dis. 27, 586-589.

Luque E., Jimena I., Noguera F., Jiménez-Reina L. and Peña J. (2002). Effects of tenotomy on regenerating anterior tibial muscles in rats. Basic Appl. Myol. 12, 203-208.

Mann C.J., Perdiguero E., Kharraz Y., Aguilar S., Pessina P., Serrano A.L. and Muñoz-Cánoves P. (2011). Aberrant repair and fibrosis development in skeletal muscle. Skelet Muscle 1, 21.

Mizuno H. (2010). The potential for treatment of skeletal muscle disorders with adipose-derived stem cells. Curr. Stem Cell Res. Ther. 5, 133-136.

Mizuno H., Zuk P.A., Zhu M., Lorenz P., Benhaim P. and Hedrick M.H. (2002). Myogenic differentiation by human processed lipoaspirate cells. Plast. Reconstr. Surg. 109, 199-209.

Noah E.M., Winkel R., Schramm U. and Kühnel W. (2002). Impact of innervation and exercise on muscle regeneration in neovascularized muscle grafts in rats. Ann. Anat, 184, 189-197.

Ostrovidov S., Hosseini V., Ahadian S., Fujie T., Parthiban S.P., Ramalingam M., Bae H., Kaji H. and Khademhosseini A. (2014). Skeletal muscle tissue engineering: methods to form skeletal myotubes and their applications. Tissue Eng. Part B Rev. 20, 403-436.

Ostrovidov S., Ahadian S., Ramon-Azcon J., Hosseini V., Fujie T., Parthiban S.P., Shiku H., Matsue T., Kaji H., Ramalingam M., Bae H. and Khademhosseini A. (2017). Three-dimensional co-culture of C2C12/PC12 cells improves skeletal muscle tissue formation and function. J. Tissue Eng. Regen. Med. 11, 582-595.

Pantelic M.N. and Larkin L.M. (2018). Stem cells for skeletal muscle tissue engineering. Tissue Eng. Part B Rev. 24, 373-391.

Peng H. and Huard J. (2004). Muscle-derived stem cells for musculoskeletal tissue regeneration and repair. Transpl. Immunol. 35, 184-192.

Peña J., Luque E., Noguera F., Jimena I. and Vaamonde R. (2001). Experimental induction of ring fibers in regenerating skeletal muscle. Pathol. Res. Pract. 197, 21-27.

Peña J., Luque E., Jimena I., Noguera F., Castilla S. and Vaamonde R. (2005). Abnormalities in tenectomized muscle fiber repair. Eur. J. Anat. 11, 37-45.

Qazi T.H., Mooney D.J., Pumberger M., Geissler S. and Duda G.N. (2015). Biomaterials based strategies for skeletal muscle tissue engineering: existing technologies and future trends. Biomaterials 53, 502-521.

Quarta M., Cromie M., Chacon R., Blonigan J., Garcia V., Akimenko I., Hamer M., Paine P., Stok M., Shrager J.B. and Rando T.A. (2017). Bioengineered constructs combined with exercise enhance stem cell-mediated treatment of volumetric muscle loss. Nat. Commun. 8, 15613.

Salvatori G., Lattanzi L., Coletta M., Aguanno S., Vivarelli E, Kelly R, Ferrari G, Harris A.J., Mavilio F., Molinaro M. and Cossu G. (1995). Myogenic conversion of mammalian fibroblasts induced by differentiating muscle cells. J. Cell Sci. 108, 2733-2739.

Sanes J.R. (2003). The basement membrane/basal lamina of skeletal muscle. J. Biol. Chem. 278, 12601-12604.

Satoh A., Labrecque C. and Tremblay J.P. (1992). Myotubes can be formed within implanted adipose tissue. Transplant. Proc. 24, 3017-3019.

Schäffler A. and Büchler C. (2007). Concise review: adipose tissue-derived stromal cells-basic and clinical implications for novel cell-based therapies. Stem Cells 25, 818-827.

Shier W.T. (1988). Studies on the mechanisms of mammalian cell killing by a freeze-thaw cycle: conditions that prevent cell killing used nucleated freezing. Cryobiology 25, 110-120.

Sicari B.M., Agrawal V., Siu B.F., Medberry C.J., Dearth C.L., Turner N.J. and Badylak S.F. (2012). A murine model of volumetric muscle loss and a regenerative medicine approach for tissue replacement. Tissue Eng Part A. 18, 1941-1948

Sicari B.M., Dearth C.L. and Badylak S.F. (2014). Tissue engineering and regenerative medicine approaches to enhance the functional response to skeletal muscle injury. Anat. Rec. (Hoboken) 297, 51-64.

Sicari B.M., Dziki J.L. and Badylak S.F. (2015). Strategies for functional bioscaffold-based skeletal muscle reconstruction. Ann. Transl. Med. 3, 256.

Spinazzola J.M. and Gussoni E. (2017). Exosomal small talk carries strong messages from muscle stem cells. Cell Stem Cell. 20; 1-3.

Takeuchi K., Hatade T., Wakamiya S., Fujita N., Arakawa T. and Miki A. (2014). Heat stress promotes skeletal muscle regeneration after crush injury in rats. Acta Histochem. 116, 327-334

Turner N.J. and Badylak S.F. (2012). Regeneration of skeletal muscle. Cell Tissue Res. 347, 759-774.

Vignaud A., Hourdé C., Torres S., Caruelle J.P., Martelly I., Keller A. and Ferry A. (2005). Functional, cellular and molecular aspects of skeletal muscle recovery after injury induced by snake venom from *Notechis scutatus scutatus*. Toxicon 45, 789-801.

Ward C.L., Ji L. and Corona BT. (2015). An autologous muscle tissue expansion approach for the treatment of volumetric muscle loss. BioResearch Open Access 4, 198-208.

Ward C.L., Pollot B.E., Goldman S.M., Greising S.M., Wenke J.C. and Corona B.T. (2016). Autologous minced muscle grafts improve muscle strength in a porcine model of volumetric muscle loss injury. J. Orthop. Trauma. 30, e396-e403.

Wong D.E., Banyard D.A., Santos P.J.F., Sayadi L.R., Evans G.R.D. and Widgerow A.D. (2019). Adipose-derived stem cell extracellular vesicles: A systematic review. J. Plast. Reconstr. Aesthet. Surg. 72, 1207-1218.

Accepted September 12, 2019